

# Multiphysics Analysis of Automotive Components for Product Portfolio Optimization

Santiago José Javier Torres García<sup>1</sup>, Eduardo David Berdeal Zertuche<sup>2</sup>, Ramiro Elizondo Villarreal<sup>3</sup>, Gabriela Margarita Martínez Cázares<sup>4</sup>

<sup>1</sup>Escuela de Ingeniería y Tecnología, Universidad de Monterrey. Email: [santiago.torres@udem.edu](mailto:santiago.torres@udem.edu)

<sup>2</sup>Escuela de Ingeniería y Tecnología, Universidad de Monterrey. Email: [eduardo.berdeal@udem.edu](mailto:eduardo.berdeal@udem.edu)

<sup>3</sup>Escuela de Ingeniería y Tecnología, Universidad de Monterrey. Email: [ramiro.elizondov@udem.edu](mailto:ramiro.elizondov@udem.edu)

<sup>4</sup>Corresponding author: [gabriela.martinezc@udem.edu](mailto:gabriela.martinezc@udem.edu)

## 1 Abstract

In this study, the pillars A, B and C from the Body-in-White (BIW) of a pickup passenger vehicle were considered, and the steels used for these components were identified based on the A2MAC1 platform, the SAEJ2947 standard, and state-of-the-art literature. Subsequently, these steels were compared with the client's product portfolio to propose a steel that meets the characteristics demanded by the automotive market for each of the components considered in the BIW. Next, the performance of each of the three pillars with these steels was validated and compared through crashworthiness simulations using Finite Element Analysis (FEA) with ANSYS LS-DYNA software. These simulations modeled the behavior of the pillars on side impact tests, with meshed parts based on the 2014 Chevrolet Silverado 1500 FEA model from the CCSA of the George Mason University. The impact speed was based on the Oblique pole side impact testing protocol from Euro NCAP; the time simulation was based on the Side impact Crashworthiness Evaluation 2.0 Rating Guidelines from the IIHS. To compare materials' behavior, different curves were defined for each case. The tested materials were evaluated by comparing internal energy and displacement on each of the three pillars. Finally, results regarding the behavior of the different materials were discussed.

**\*KEYWORDS:** BIW, Automotive steels, Crashworthiness, FEA, Virtual validation, A-pillar, B-pillar, C-pillar.

## 2 Introduction

In recent years, the automotive industry has made significant advances in the research of new steels for automotive applications, as well as in the optimization of their designs. The continuous pursuit of these improvements is primarily based on the goal of increasing vehicle efficiency and reducing fuel consumption to mitigate the rise in carbon dioxide emissions, without compromising passenger safety.

To achieve these objectives, the new materials must meet the high standards demanded by the industry, fulfilling requirements in critical areas such as safety, environmental impact, manufacturing, economy, quality, and durability. Currently, steel accounts for an average of 65% of a vehicle's total weight. Therefore, reducing even 1% of this weight results in a 0.5% decrease in fuel consumption [22]. On the other hand, Demeri estimates that a 10% reduction in vehicle weight can lead to a 6–8% improvement in fuel efficiency [3].

Specifically, efforts are focused on reducing the weight of the Body-in-white (BIW) structure rather than other areas of the vehicle, such as passenger comfort systems or the powertrain, since compromising these systems could negatively affect the vehicle's market value [11].

Similarly, cost plays a fundamental role in selecting a material for automobile manufacturing, encompassing aspects ranging from design, raw materials, and manufacturing processes to the tests these materials must undergo. In terms of safety, automotive manufacturers focus on two key concepts: the energy absorption potential in the event of an impact and resistance to the penetration of projectiles or fragments [14].

In summary, the automotive industry is constantly evolving to achieve better efficiency, safety, and profitability in its vehicles, which entails investing in research into new technologies and materials. With the increasing demand for lightweight and durable materials for vehicle manufacturing, companies must align their product portfolios with market trends.

## 2.1 General Objective

The general objective of this study is to propose a multi-physical analysis model for the characterization and validation of automotive steels, which will support decision-making related to the product portfolio of Company X.

## 2.2 Specific objectives

1. Identify market trends in steels for specific BIW components.
2. Propose and apply virtual validation tests for trending steels.

## 3 Background

Safety is a crucial factor in the automotive industry. Consumers expect cars to be safe, which is why governments are demanding new tests and standards within companies that influence structures, designs, and materials to meet this criterion. There are two key safety concepts to consider: impact resistance and penetration resistance. Impact resistance is defined as the energy absorption potential through controlled failure mechanisms that provide a gradual reduction in the load profile during absorption, while penetration resistance deals with total absorption without allowing projectiles or fragments to penetrate the material. This is why various organizations worldwide are dedicated to measuring vehicle safety; among them is the National Highway Traffic Safety Administration (NHTSA), which sets vehicle safety standards, such as impact resistance, restraints, and fuel economy. Similarly, the European New Car Assessment Program (NCAP) measures vehicle performance in a variety of crash tests, including frontal, side, pole, and pedestrian impacts [10], [14].

### 3.1 Steels in the automotive industry

Research in the automotive industry aims to meet four global objectives: reducing pollutant gas emissions; improving fuel efficiency; increasing and ensuring passenger safety; and reducing manufacturing costs. In general, the materials involved in this pursuit must have the ability to resist deformation and absorb impact energy. This is broken down into the properties of automotive materials, which include stiffness, tensile strength, hardening, fatigue resistance, crashworthiness, formability, and toughness.

Over the years, steel has proven to be a suitable alternative when selecting materials for automotive manufacturing, given its relatively high formability, corrosion resistance (with zinc), ease of joining, recyclability, and energy absorption capacity from impacts [14]. Other favorable points of steel include its high yield range, stiffness, and low cost: thanks to these characteristics, it can be considered an appropriate material for producing lighter, stronger vehicles with greater efficiency and passenger safety [14].

In general, next-generation steels do not offer a lighter alternative due to having lower density but, because of their strength properties, they can be used in thinner gauges, which is where weight reduction is achieved [3].

### 3.2 Classification of automotive steels

In the automotive industry, there are various ways to classify steels. One method is metallurgical designation, which provides certain information about the process. Common designations include low-strength steels (interstitial-free and mild steels), conventional high-strength steels (HSS) such as high-strength low-alloy steels (HSLA), and advanced high-strength steels (AHSS).

Since the classification methods for steels vary considerably, the WorldAutoSteel format will be used to define them, where each steel grade is identified by its metallurgy, minimum yield strength and minimum tensile strength (in MPa) [10].

#### 3.2.1 Conventional steels

**Mild steels** generally exhibit relatively low resistance to deformation but have good formability and low cost [16]. They are typically low in carbon and do not contain alloying elements for reinforcement, resulting in a relatively lower yield strength compared to other steel groups [20]. However, their total elongation percentage, or ductility, is higher than that of other steels due to their primarily ferritic microstructure. Their microstructure may also contain pearlite, depending on the carbon content. Applications of mild steels in automotive bodies include auxiliary parts and locks [16], [8].

**Bake Hardenable (BH)** steels usually present a balanced combination of strength and formability [3]. This is achieved through the diffusion of interstitial carbon and nitrogen, which increases the yield

strength [3] without affecting formability [10]. This occurs because carbon remains in solution during initial processing, then precipitates out during paint baking [10]. These steels are commonly found in external automotive components where dent resistance is required [10]. In short, the bake hardening effect can be described as the increase in yield strength after forming a part, without affecting formability, with values ranging from 40 to 90 MPa [7].

**High-Strength Low-Alloy (HSLA)** steels, better known as HSLA, have a low carbon content (<0.3% C), and approximately 1% or less of alloying elements (manganese, phosphorus, chromium, nickel, silicon, and molybdenum) are added to low-carbon steels (0.02 to 0.13% C) to achieve high strength levels. Their microstructure consists of two phases: fine-grained ferrite and hard martensite and austenite. High strength is achieved through rapid cooling, producing very fine ferrite. Grain size is refined by solid solution strengthening with phosphorus, nitrogen, silicon, and manganese, and carbide formation with vanadium, nickel, and titanium. Additionally, their yield strength without heat treatment is above 485 MPa. This class of steels has low formability and is used in the body-in-white and structural applications beneath the body where strength is needed to increase service loads [11], [14].

### 3.2.2 AHSS: first generation

The standout property of **ferritic-bainitic (FB)** steels is localized formability, which can be measured through hole expansion tests. This property is generally due to three factors: the presence of bainite in addition to ferrite, fine grain size, and minimal difference in the hardness of the two phases present in the microstructure [19]. Additionally, this property, measured as edge expansion, places FB steels above DP and HSLA steels [19], as well as being considered first-generation advanced steel (as of 2021, according to WorldAutoSteel [19]), since these steels exhibit combined strength and formability properties [15]. In automobiles, these steels can be found in structural parts like suspension control arms, seat supports, and longitudinal beams [19].

A notable feature of **Transformation-Induced Plasticity (TRIP)** steels is that they offer a unique combination of high strength and high formability [6]. The TRIP effect consists of the transformation of retained austenite to martensite during plastic deformation [3]. Their significant advantage is that, although they have similar tensile strength to other steels, they exhibit considerably higher ductility [3]. Their applications include components that can absorb energy through deformation, such as cross members in the front and rear areas of vehicles [8].

**Dual-Phase (DP)** steels are duplex steels with a microstructure consisting of a soft ferrite matrix and 10% to 40% volume of martensite islands. Their strength comes from the martensitic phase, while their ductility comes from the ferritic phase. This type of microstructure allows them to achieve ultimate tensile strength in the range of 500 to 1200 MPa. Due to their excellent combination of strength and ductility, they are widely used in the automotive industry. Additionally, they have a higher initial hardening rate and a lower ratio of tensile strength to yield strength compared to High-Strength Low-Alloy (HSLA) steels of similar strength.

**Martensitic Steels (MS)** are obtained by transforming austenite into martensite during the quenching process. This transformation begins during cooling when austenite reaches the martensite start temperature ( $M_s$ ). As the temperature decreases, more of the austenite transforms into martensite, and finally, when the martensite finish temperature ( $M_f$ ) is reached, the transformation is complete, resulting in a matrix composed of martensite with small amounts of ferrite and/or bainite [3].

These steels are notable for their high tensile strength, reaching up to 1700 MPa of ultimate tensile strength. Typical applications of MS steels include those requiring high strength and good fatigue resistance, with relatively simple shapes for traditionally stamped parts and more complex shapes for hot-formed parts. Typical applications of MS steels include bumper reinforcements, door intrusion beams, side sill reinforcements, and, more recently, shaped rocker panel reinforcements [10], [3].

**Press-Hardened Steels (PH)** are commonly composed of carbon-manganese-boron. These steels have a ferrite-pearlite microstructure and a yield strength between 300-600 MPa, depending on the amount of cold work. Tensile strength tends to be between 450 and 750 MPa. Elongation should exceed 12% (A80), but depending on the type of coating and thickness, it can exceed 18% (A80) [15]. When hardened, it has a minimum yield strength of 950 MPa and tensile strength ranging from 1300 to 1650 MPa. PH steels are applied in the automotive industry, such as in A and B pillars, EV battery protectors, sill reinforcements, cross members including roof panels, and door reinforcements [21].

### 3.2.3 AHSS: second generation

The main characteristic of **TWIP** (Twinning-Induced Plasticity) steels is the high manganese content as an alloying element. Manganese significantly reduces the transformation temperature from austenite to ferrite [3]. This means that the steel can be 100% austenitic at room temperature. The twins act as deformation barriers. These barriers function like grain boundaries, making the microstructure finer and gradually increasing resistance to deformation, which translates into a high strain hardening exponent [10]. One of the most important applications of these steels is their use in automotive deformation zones, as they absorb relatively high levels of energy due to their high strain hardening exponent. In simple terms, these steels combine high strength with high levels of energy absorption, elongation, and strain hardening.

The properties of each of these steels can be achieved through a combination of alloying elements and heat treatments. Both factors, together with manufacturing processes, generate the microstructural phases that give steels their different mechanical properties. In general, high cooling rates favor the formation of austenite to martensite, and lower cooling rates result in more ferrite formation [3]. On the other hand, alloying elements generally have the ability to modify the temperatures and phase transformation times.

## 3.3 BIW and Crashworthiness

### 3.3.1 BIW and cabin pillars

In 2010, 60% of the weight of a "light" vehicle was made up of steel [3]. Specifically, efforts are focused on reducing weight in the Body-in-white (BIW) structure rather than in other areas of the vehicle, such as passenger comfort systems or the powertrain, as compromising these systems could negatively affect the vehicle's market value [11]. On the other hand, BIW components account for approximately 30% of a vehicle's weight [17].

Essentially, the potential to reduce weight with a given steel is measured by considering its resistance to deformation; furthermore, the combination of strength + ductility and the energy absorption capacity can be predicted by understanding the microstructure of that steel [7].

**The A-pillar** is one of the components in the cabin zone responsible for passenger safety. It is located on the side of the front of the vehicle, before the driver and passenger doors. Generally, it is made up of an upper part and a lower part, along with their reinforcements.

**The B-pillar** is one of the most important parts for ensuring passenger safety and is also located in the cabin zone. It is positioned on the side of the vehicle, between the front and rear doors. Typically, it is made from a single piece of martensitic or press-hardened steel (PH), as it must provide high resistance against cabin intrusion.

**The C-pillar** is the safety component of the cabin located behind the rear door. Along with the A and B pillars, it forms the cabin zone and protects passengers from side impact intrusions. These three components are usually made of steels with high resistance to deformation, in order to fulfill the role of protecting passengers.

### 3.3.2 Crashworthiness

The term *crashworthiness* refers to the ability of a vehicle, or a component, to absorb energy by dissipating the applied load [14]. More generally, the goal of studying crashworthiness is to optimize the distribution of energy throughout the vehicle after an impact, in such a way that the energy received by the passengers is minimized [4]. Thus, impact energy can be absorbed through deformation of the component or redirected to the passenger safety systems, depending on the area to which the component belongs: the cabin zone or the deformation zone.

The cabin zone must not allow deformations or intrusions that could compromise passenger safety during an impact. To achieve this, materials used in components of this zone must have high strength (the highest possible yield strength [7]), which is why MS, PH, and DP steels (>980 MPa) are suitable for such components [10], [16]. There is even talk of steels with UTS (ultimate tensile strength) close to 1800 MPa for anti-intrusion applications [3]. The steels in this zone form components such as the A, B, and C pillars, which must have considerable intrusion resistance.

On the other hand, the deformation zones must absorb as much energy as possible through elongation, cushioning the impact. In this way, even though the car may be heavily deformed after a crash, the energy of deformation is not absorbed by the passengers. For this purpose, materials in this zone must be able to absorb energy through deformation, which can be achieved through mechanical properties such as work hardening capacity and a combination of strength and ductility (toughness), which can be seen as a larger area under the material's stress-strain curve [3], [7], [14], [16]. A high work hardening rate indicates that the material becomes stronger with the impact, absorbing energy [3]. Typically, steels that can fulfill this purpose belong to the DP, CP, and TRIP groups [10], due to their combined properties of strength and ductility, as well as work hardening capacity [16]. Both the front and rear zones of the vehicle must be deformable to contain the kinetic energy of the crash [4]; these zones are designed "like an accordion" to absorb the impact force [3].

Virtual crashworthiness simulations are used to estimate the behavior of vehicles or their components during an impact, quickly and with relative accuracy, without moving directly to physical testing. These simulations use multiple numerical tools, such as the Finite Element Method (FEM). The models for these simulations must be reliable, robust, and easy to build and run [4]. Since multiple changes can be made during simulations and they generally involve many iterations, the model must be able to run relatively quickly. Additionally, these simulations can show the behavior of the vehicle at the assembly level or by analyzing the response of individual components, such as those that make up the BIW.

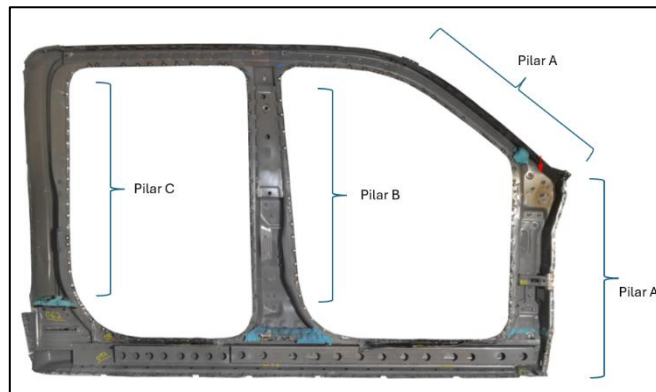


Fig. 1: BIW pillars A, B and C. Image taken from A2MAC1 platform.

Component	Function	Steels used
A-Pillar	Bending stiffness, NVH (Noise, Vibration, Harshness), manufacturability, durability [11]	TWIP 500/900 [10], HF [10]
B-Pillar	Bending stiffness, NVH, manufacturability, durability [11], Impact resistance	HF 1050/1500 [10], [6], TWIP 500/980 [10], MS 950/1200 [6]
C-Pillar	Torsional stiffness [18]	Hot-stamped 1550 with boron [1]

Table 1: BIW pillars.

## 4 Methodology

To understand the methodology applied in this project, it is essential to examine the platforms used, the standards that justify the results, and the simulation software employed.

### 4.1 A2MAC1

A2MAC1 is a reference platform in the field of automotive engineering, primarily known for its extensive automotive benchmarking database. It provides detailed information and comparative analyses of vehicles and their components, allowing users to access data regarding material types, mechanical

properties, and chemical composition of various vehicles on the market. This enables engineers to conduct thorough analyses of market trends.

#### 4.2 SAEJ2947

This standard includes steel grades currently available and used in the automotive industry, ranging from low-carbon mild steel sheets to advanced high-strength steel (AHSS) sheets. It establishes and defines the requirements for continuous casting automotive steel grades that can be formed, welded, assembled, and painted in automotive manufacturing processes [13].

#### 4.3 Euro NCAP (Oblique Pole Side Impact)

The Euro NCAP (European New Car Assessment Programme) is a standard that establishes the necessary parameters for simulating a side-impact crash. In this test, a car is propelled laterally at 32 km/h into a rigid, narrow pole. This test is highly severe and assesses the vehicle's ability to protect the driver's head. Due to the localized nature of the load on the vehicle, deformation can be significant, and the pole may deeply penetrate the cabin [5].

#### 4.4 Ansys LS-DYNA

LS-DYNA is a multiphysics process simulation software developed by Livermore Software, specializing in explicit, linear, and nonlinear analyses. LS-DYNA supports the understanding of vehicle structure deformation due to its extensive material definitions and contact modeling capabilities [12]. In this project, LS-DYNA is used as a tool to evaluate the behavior of various materials in Body-in-White (BIW) components. The evaluation is conducted through explicit Finite Element Analysis (FEA) simulations.

#### 4.5 Case study

In this study, the 2014 Chevrolet Silverado model, shown in Figure 2, was analyzed. A multiphysics analysis was conducted on the A, B, and C pillars, which are illustrated in Figure 3. The objective of this case study is to analyze the materials used in these components, verify their behavior through finite element simulations, and compare them with the steels from a specific company. The same simulation parameters were applied to the company's steel products to observe and evaluate their behavior.



Fig.2: Chevrolet Silverado 2014. Image taken from A2MAC1 platform.



Fig.3: Pillars A, B and C from Chevrolet Silverado 2014. Images taken from A2MAC1 platform.

#### 4.6 Methodological steps

1. The first step is to identify the specific steel used for each component in this model. To achieve this, the Ultimate Tensile Strength (UTS) range provided by the A2MAC1 platform is identified. Once this range is determined, a filtering process is conducted using the steels that meet this initial criterion, with the support of the SAE J2947 standard. Subsequently, after identifying the steels that satisfy this first filter, their chemical compositions are compared with those provided by the platform, further filtering by percentage similarity, and selecting the steels that meet both criteria.

2. The second step involves comparing the selected steels with the client's product portfolio to ensure that sufficient information is available to perform the multiphysics study. The necessary information for the next step includes the stress-strain curves of the client's steels.
3. Finally, a crashworthiness analysis is performed using Finite Element Analysis (FEA) on both the steels from the standard and the client's steels.

#### 4.7 Model application to A-Pillar

As shown in Table 2, it is observed that for Pillar A, a value of 578 UTS is required. Therefore, based on the standard, the steels that meet this specification are those presented in Table 3.

Material – A-pillar	
Material	Steel
HV Hardness	178
Tensile strength estimated [MPa]	578
Class	500-750 MPa

Table 2: A-Pillar. Information from A2MAC1.

UTS Range – SAEJ2947	Steel
480-600	CR460LA
520-680	CR500LA
560-720	CR550LA
480-600	HR500LA
560-700	HR550LA
490-600	CR330Y590T-DP
580-680	HR330Y580T-DP
580-700	HR440Y580T-FB

Table 3: Identified steels for A-Pillar.

For Pillar A, it was identified that the steels meeting the chemical compositions (Table 4), as specified in the standard and the A2MAC1 platform, were the HR330Y580T-DP steel and the HR440Y580T-FB steel.

Case	C%	Mn%	Cr+Mo%	Si%	Ti+Nb%	Al%	S%
A2MAC1 Steel	0.102	1.92	0.3932	0.241	0.007	0.0526	0.0017
CR500LA	≤0.13	≤1.70	-	≤0.60	≤0.25	≥0.015	≤0.025
HR500LA	≤0.12	≤1.70	-	≤0.50	≤0.25	≥0.015	≤0.025
CR290Y490T-DP	≤0.14	≤1.80	≤1.00	≤0.50	≤0.15	0.015-1.0	≤0.010
<b>HR330Y580T-DP</b>	≤0.14	≤2.20	≤1.40	≤1.0	≤0.15	0.015-1.0	≤0.010
<b>HR440Y580T-FB</b>	≤0.18	≤2.00	≤1.00	≤0.50	≤0.15	0.015-2.0	≤0.010

Table 4: Alloy elements comparison for A-Pillar.

Finally, the steels that are most similar to the A2MAC1 steels, are compared with the steels from the client's product portfolio, as it is shown in table 5.

Pillar	Selected steels	Client's steel
A	HR330Y580T-DP	Proposal #1
	HR440Y580T-FB	

Table 5: Selected steels for A-Pillar.

#### 4.8 Virtual validation of selected steels

After replicating the methodology for each pillar and identifying the appropriate steels with their proposals, crashworthiness simulations were carried out using Finite Element Analysis (FEA) in an explicit form, utilizing the LS-DYNA software. These simulations provided an initial understanding of the energy absorption profile for each pillar with the identified steels. A total of six simulations were performed. For each of the three pillars, the same test was conducted with two selected steels: one with a baseline steel proposed from literature research, and the other with the client's proposal for the pillar in question, as shown in Table 6.

Material	A-Pillar	B-Pillar	C-Pillar
<b>Material – Test #1</b>	HSLA 420-500	MS 1250-1500	HSLA 550-650
<b>Material – Test #2</b>	Proposal #1	Proposal #2	Proposal #3

Table 6: Virtual validation tests.

For each individual case, the test consisted of a side impact test, where each pillar collided at a certain speed with a rigid steel pole, as shown in Figure 13. The speed parameters were based on the 'Oblique Pole Side Impact Testing Protocol' from Euro NCAP [5]; while the test time parameters were based on the 'Side Impact Test Program' from IIHS [9].

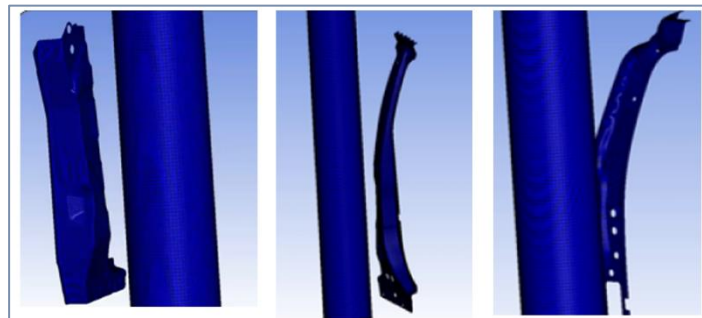


Fig.4: FEA simulations of A, B and C pillars colliding with a rigid pole.

##### 4.8.1 Meshing

The first step in developing the virtual validation was to adjust the meshes of each of the pillars, based on the finite element model of the 2014 Chevrolet Silverado created by the CCSA at George Mason University (Fig. 14) [2].

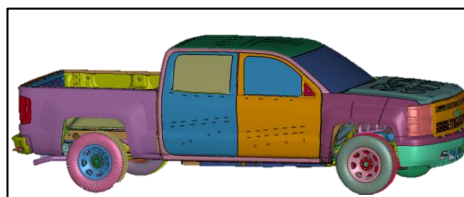


Fig.5: Chevrolet Silverado 2014 FEA model. Image from CCSA, George Mason University [2].

From this model, the meshes of the main panels of pillars A, B, and C were adjusted (Figure 6). For these tests, an average mesh size of 6 mm was considered appropriate, using first-order square shell elements. This was done to allow for a potential future study of structural optimization, where the thickness of the sheets forming the pillars could be varied. On the other hand, for ease of computational power, shell elements were chosen to be maintained instead of migrating to solid elements. The thickness measurements of the element used for each pillar were 1.5, 2.15 and 1.00 mm for the A-Pillar, B-Pillar and C-Pillar, respectively.



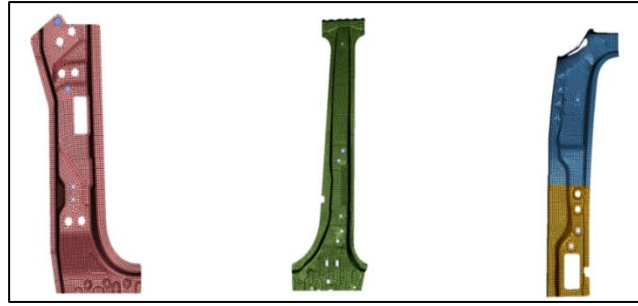


Fig.6: Meshes of A-Pillar, B-Pillar and C-Pillar.

For the rigid steel pole, a 10 mm-mesh was used, with square shell elements of thickness of 15 mm.

4.8.2 Materials and parameters

The independent variable in the tests was the material assigned to the meshes. Table 7 provides a detailed definition of the materials for each simulation. For all steels, including the material of the rigid pole, a density of 7890 kg/m<sup>3</sup> was used, along with a Young's modulus of 210 GPa and a Poisson's ratio of 0.3.

Pillar	Test #	Steel	Modelo de mat	$\sigma_y$ [MPa]
A	1	HSLA 420-500	MAT_PIECEWISE_LINEAR_PLASTICITY	420
	2	Proposal #1		535.21
B	1	MS 1250-1500	MAT_MODIFIED_PIECEWISE_LINEAR_PLASTICITY	1250
	2	Proposal #2		461
C	1	HSLA 550-650	MAT_PIECEWISE_LINEAR_PLASTICITY	550
	2	Proposal #3		526.56

Table 7: Materials definitions.

Additionally, each material was defined with a stress-strain curve that was input into the software, as shown in the following graphs.

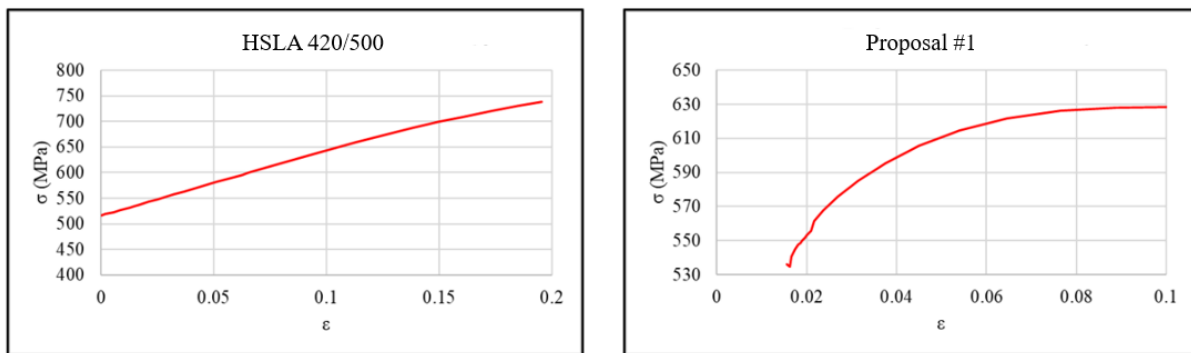


Fig.7: Stress-Strain curves for A-Pillar tests.

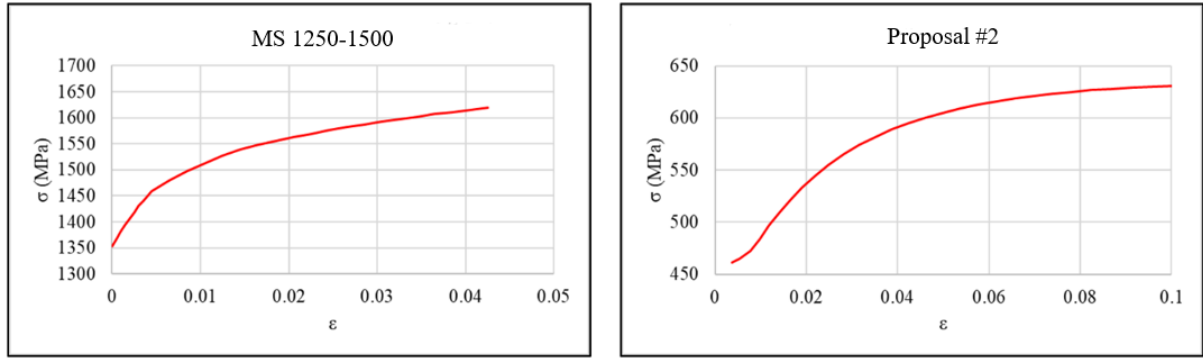


Fig.8: Stress-Strain curves for B-Pillar tests.

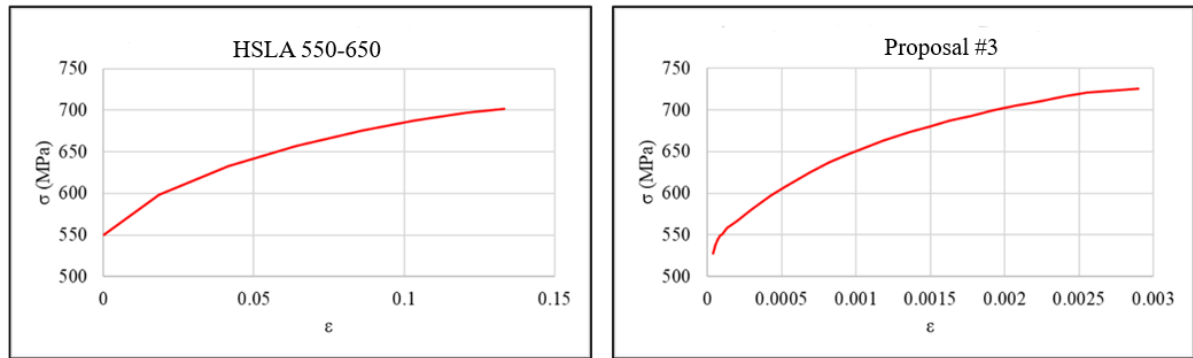


Fig.9: Stress-Strain curves for C-Pillar tests.

<b>Contacts</b>	Model	CONTACT_AUTOMATIC_SURFACE_TO_SURFACE
	Surface	Between each pillar and the pole
	Friction Coeffs.	Static: 0.2 Dynamic: 0.1
<b>Impact test parameters</b>	Velocity	32 km/h [5]
	Simulation time	0.1 s [9]
<b>Restrictions (SPC)</b>	6 DOF	Pole
	Y free displacement	Top and bottom edges of each pillar
<b>Control</b>	Energy	Hourglass
		Stonewall
		Sliding interface
		Rayleigh
		Initial ref. Geometry
		Material Energy
		Dissipation energy

Table 8: Boundary conditions and analysis definitions.

As shown in Table 8, for the constraints, 'single-point constraint' (SPC) boundary conditions were used to keep the pole completely fixed during the impacts and to ensure that the pillars, upon collision, had no rotation and only displacement along the Y-axis. In the case of energies, all types were considered in the balance, except for 'drilling' energy.

5 Results

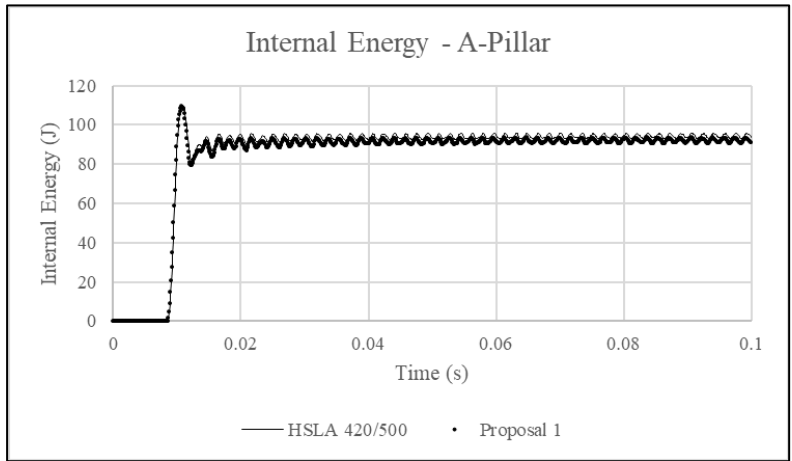


Fig.10: Internal Energy for A-Pillar.

In Figure 10, a very close correlation in the energy absorption of both materials can be observed. This may be due to the similarity in both the material definition curves and the yield strength (YS) definition. This confirms that the client's steel exhibits behavior similar to what is expected from the literature.

A-Pillar: test	A-Pillar: proposal	Pole	Simulation
Material: HSLA 420/500	Material: Proposal #1	Material: rigid steel	Time: 0.1 s
Mass: 2.994 kg		Mass: 189.57 kg	Speed: 32 km/h

Table 9: FEA simulation parameters for A-Pillar.

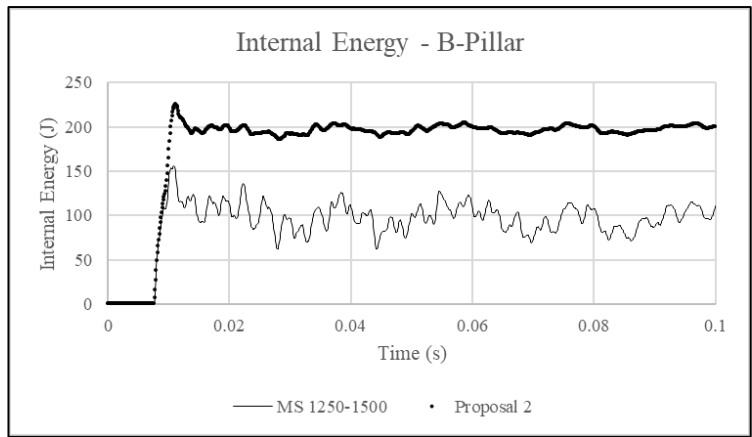


Fig.11: Internal Energy for B-Pillar.

It can be observed that the energy absorption profile in the B pillar is generally higher than in the A pillar, which may be due to the geometry of the pillar as well as the thickness of the part. On the other hand, in terms of materials, it can be seen that the steel that absorbs the most energy is the client's, which makes sense due to its lower yield strength and a curve with higher toughness. However, this is not a determining factor in the use of this specific steel for this pillar, as the tests were carried out using the client's information about the available steels, which should not necessarily be considered as the optimal option. Furthermore, specifically speaking about the B pillar, it is indeed more likely that the material used would be martensitic steel, given the deformation resistance that this component must exhibit. Therefore, even though its energy absorption profile may seem inconsistent, this is not a reason to completely rule out MS 1250-1500 steel as a material option for this component. On the other hand, it is important to notice that steels like DP, due to their chemical compositions, can be hardened and

converted to PH steels or MS steels, with hot stamping process, but this depends on the steel's chemical composition.

B-Pillar: test	B-Pillar: proposal	Pole	Simulation
Material: MS 1250-1500	Material: Proposal #2	Material: rigid steel	Time: 0.1 s
Mass: 7.143 kg		Mass: 189.57 kg	Speed: 32 km/h

Table 10: FEA simulation parameters for B-Pillar.

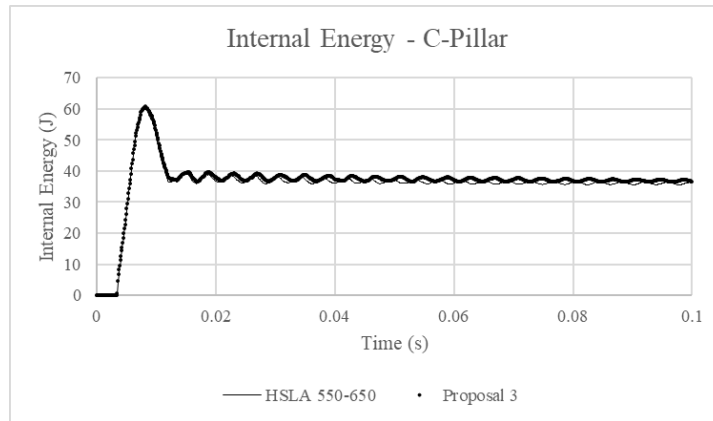


Fig. 12: Internal Energy for B-Pillar.

The case of the tests for the C pillar shows results quite similar to those of the A pillar tests, not in terms of the absolute amount of energy absorption, but in the close relationship between both materials in each test. Again, this can be attributed to the similar yield strengths as well as the similarities in the stress-strain curves, which again indicates that the client's material may exhibit behavior similar to what would be expected according to the literature.

C-Pillar: test	C-Pillar: proposal	Pole	Simulation
Material: HSLA 550/650	Material: Proposal #3	Material: rigid steel	Time: 0.1 s
Mass: 1.706 kg		Mass: 189.57 kg	Speed: 32 km/h

Table 11: FEA simulation parameters for C-Pillar.

## 6 Summary

- Steel is a material that is constantly evolving. Due to properties such as strength, stiffness, and cost, it will continue to be a trending structural material.
- It is possible to design the mechanical properties of steel through metallurgical design, chemical composition, and appropriate heat treatment to achieve the necessary microstructure for any component. On the other hand, hardenability of steel can be improved with alloying elements.
- Innovation and design of automotive steels, using heat treatments, have allowed for the same or better mechanical properties in components, with reduced thickness.
- In the virtual validation of the applied case study, a very close correlation in energy absorption behavior was achieved for the steels in the A and C pillars. Nevertheless, these simulations can be further developed, optimizing mesh sizes and considering the mass of more parts of the vehicle.
- The developed model to characterize steels is functional and replicable for any component and customer material.

## 7 Literature

[1] Chen, G: "Optimized Design Solutions for Roof Strength Using Advanced High Strength Steels," SAE International, 2010.

- [2] CCSA - George Mason University: "2014 Chevrolet Silverado 1500 Detailed Finite Element Model," Accessed: Apr. 19, 2024.
- [3] Demeri, M. Y: "Advanced high-strength steels: science, technology, and applications," 2013.
- [4] Du Bois, P: "VEHICLE CRASHWORTHINESS AND OCCUPANT PROTECTION Automotive Applications Committee American Iron and Steel Institute Southfield, Michigan," 2004.
- [5] Euro NCAP, "EUROPEAN NEW CAR ASSESSMENT PROGRAMME (Euro NCAP) OBLIQUE POLE SIDE IMPACT TESTING PROTOCOL", 2023. Accessed: May 01, 2024. [Online]. Available: <https://www.euroncap.com/media/79876/euro-ncap-pole-protocol-oblique-impact-v72.pdf>
- [6] Eroğlu, M: "Advanced High Strength Steels (AHSSs): Production and Applications," 2019.
- [7] Fonstein, N: "Advanced High Strength Sheet Steels: Physical Metallurgy, Design, Processing, and Properties," 2015.
- [8] Hu, X. and Feng, Z: "Advanced High-Strength Steel-Basics and Applications in the Automotive Industry," 2021.
- [9] IIHS: "IIHS Side Impact Test Program Rating Guidelines," 2016. Accessed: May 01, 2024.
- [10] Keeler, S., Kimchi, M., and Mooney, P. J: "Advanced High-Strength Steels Application Guidelines Version 6.0," WorldAutoSteel, 2017.
- [11] Mayyas, A., et al: "Using Quality Function Deployment and Analytical Hierarchy Process for material selection of Body-In-White," Mater Des, vol. 32, no. 5, pp. 2771–2782, May 2011, doi: 10.1016/j.matdes.2011.01.001.
- [12] Oasys: "LS-DYNA®." Accessed: May 13, 2024.
- [13] SAE: "SAEj2947."
- [14] Singh, M., Wwww, W., and Singh, M. K: "Application of Steel in Automotive Industry International Journal of Emerging Technology and Advanced Engineering Application of Steel in Automotive Industry," 2016. [Online]. Available: [www.ijetae.com](http://www.ijetae.com).
- [15] Society of Automotive Engineers: "Categorization and Properties of Steel Sheet for Automotive Cold Forming Applications," Apr. 2022.
- [16] Tamarelli, C. M: "AHSS 101 THE EVOLVING USE OF ADVANCED HIGH-STRENGTH STEELS FOR AUTOMOTIVE APPLICATIONS," 2011. [Online]. Available: [www.autosteel.org](http://www.autosteel.org).
- [17] Taylor, T. and Clough, A: "Critical review of automotive hot-stamped sheet steel from an industrial perspective," May 03, 2018, Taylor and Francis Ltd. doi: 10.1080/02670836.2018.1425239.
- [18] Valladares, D., et al: "Development of a new car C-pillar made of sandwich structures," Journal of Sandwich Structures and Materials, vol. 23, no. 6, pp. 2586–2613, Sep. 2021, doi: 10.1177/1099636220909947.
- [19] WorldAutoSteel: "Ferrite-Bainite." Accessed: May 07, 2024.
- [20] WorldAutoSteel: "Mild Steels." Accessed: May 06, 2024.
- [21] WorldAutoSteel: "Press hardened steels." Accessed: May 12, 2024.
- [22] Yerania, G: "CORPORACIÓN MEXICANA DE INVESTIGACIÓN EN MATERIALES," 2009.